Aalborg Universitet

AALBORG UNIVERSITY
DENMARK

Harmonic Interaction Analysis in Grid Connected Converter using Harmonic State Space (HSS) Modeling

Kwon, Jun Bum; Wang, Xiongfei; Bak, Claus Leth; Blaabjerg, Frede

Harmonic Interaction Analysis in Grid Connected Converter using Harmonic State Space (HSS) Modeling

JunBum Kwon, Xiongfei Wang, Claus Leth Bak, Frede Blaabjerg
Department of Energy Technology
Aalborg University
Aalborg, Denmark
E-mail : {jbk, xwa, clb, fbl} @et.aau.dk

Abstract - An increasing number of power electronics based Distributed Generation (DG) systems and loads generate coupled harmonic as well as non-characteristic harmonic with each other. Several methods like impedance based analysis, which is derived from conventional small signal- and average-model, are introduced to analyze these problems. However, it is found that Linear Time Invariant (LTI) base model analysis makes it difficult to analyze these phenomenon because of time varying system operation trajectories, varying output impedance seen by grid connected systems and neglected switching component during the modeling process. This paper investigates grid connected converter by means of Harmonic State Space (HSS) small signal model, which is modeled from Linear Time varying Periodically (LTP) system. Further, a grid connected converter harmonic matrix is investigated to analyze the harmonic behavior interaction and dynamic transfer procedure. Frequency domain as well as time domain simulation results are represented by means of HSS modeling to verify the theoretical analysis. Experimental results are also included to validate the method.

I. INTRODUCTION

With the increased utilization of power electronics based Distributed Generation (DG) System, the harmonic stability and dynamic harmonic performance in the system is an important issue in today [1-5]. Particularly, DG systems are gathered into the same grid network, where complex connection and active control of each converter can make it difficult to analyze the non-linear dynamics and harmonic interaction of power electronics based systems [2, 6-10]. These unpredicted harmonic components in the system, which are generated from the interaction from other systems, may lead to instability problems in the power electronics based systems [4, 11]. To analyze these problems, some methods like impedance based analysis, which is derived from small signal- and average-model, are introduced [4, 12-14]. However, in different cases, Linear Time Invariant (LTI) base model analysis is not enough to analyze these phenomenon because of time varying system operation, varying output impedance seen by grid connected systems and the

neglected switching component during the modeling process. Hence, detailed analysis of the harmonic interaction based on the grid network as well as the power electronics based system are fundamentally required in order to stabilize the power converters in the same grid network [4, 5, 11].

In order to solve the problems, which can not be analyzed by the conventional methods, some new approaches considering periodical signals concept have been carried out. In order to calculate the input-output impedance of 3-phase systems according to the linearized sequence components, a harmonic linearization method is introduced [15, 16]. In another case, steady state analysis of Modular Multilevel Converter (MMC) is performed to analyze the circulating current by means of Fourier series expression and small signal-modeling [17, 18]. However, harmonic interaction with an overall picture of other components is not studied. Furthermore, the harmonic interaction problem inside the voltage source converter is overlooked due to a simplified modeling approach, where most of the modeling methods are assuming the converter to be operated at fixed operating point [19].

To analyze these harmonic couplings at the transmission level, Harmonic Domain (HD), Extended Harmonic Domain (EHD) and Harmonic State Space (HSS) modeling method was introduced in power delivery system analysis. For the steady-state harmonic coupling investigation both in symmetrical and unsymmetrical grid condition, the harmonic domain method is developed [20]. By considering the analyzed dynamic results from the steady-state results, EHD modeling is introduced in order to reduce the simulation time [21]. However, this approach is not enough to derive the dynamic performance and to consider the switching instant variation. As a result, the HSS modelling method is developed to meet the overall requirement including harmonic interaction and inter-harmonic analysis possibilities [22-26].

This paper presents a comprehensive analysis on the effect of harmonic interaction in terms of grid connected converter by means of HSS modeling. Based on this method, the harmonic transfer as well as interaction of grid connected converters is
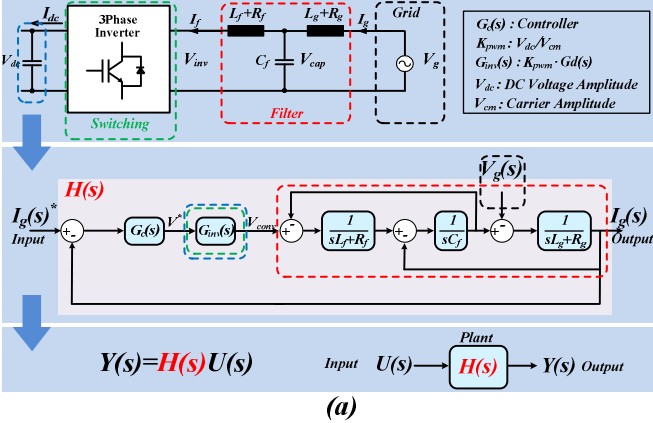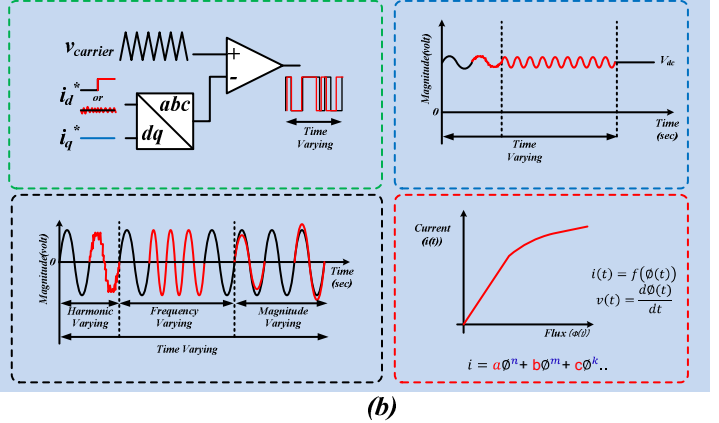
Fig 1. Block diagram of modeling approach (a) Linear Time Invariant (*LTI*) model (b) Block diagram of Non-linear / Time varying elements

analyzed with the grid voltage states according to the international standards including symmetrical and non-symmetrical characteristics. Additionally, possible harmonic interaction among the components is investigated. Lastly, simulation and experimental results are included to validate the proposed theoretical analysis method.

II. PROBLEMS OF TIME INVARIANT MODEL BASED ANALYSIS

The general procedure to analyze the grid connected inverter is shown in Fig. 1. However, practically, the Grid connected Voltage Source Converter (*GVSC*) can be represented into non-linear and time-varying differential equation. To neglect those two components in the *LTI* model, some assumptions are needed.

1) "*Every passive component*" (Fig. 1 – red box) operates in the linear region of the component characteristics. In the case of a very simple circuit with an inductor, if the current rating is higher than the linear region, the differential equation will be a non-linear. However, the only linear part is considered according to the assumption that the inductor is well designed.

2) "*DC link capacitor*" is sufficiently large as well as the voltage is always constant (Fig. 1 – blue box). If the dc-link voltage controller is considered, it is hard to analyze the stability criterion because of the multiple input/output. Hence, to be convenient for the analysis, most of the state-space averaged base small signal model [9] is focusing on the filter and controller performance instead of the disturbance from the outside of the converter. However, the dc-link voltage is varying, when the dc-dc converter or Back to Back (BtB) are connected to the dc link voltage.

3) "*Switching and switch characteristic*" (Fig. 1 – green box) are generally neglected in the model. To make the *LTI* system model, magnitude of the carrier signal is only taken into account in the analysis model without considering the PWM method according to the assumption, where the reference signal (V^*)

from controller is fixed at a specific point. This assumption is normally available, when the Fourier coefficient of the PWM is not quite varied because of a high-carrier switching frequency.

4) "*Grid voltage variation*" (Fig. 1 – black box) is not only regarded as pure sinusoidal signal in the *LTI* model, but also neglected in the analysis under the assumption, where it will not generate any disturbance. However, actually, the grid voltage is a time varying signal because of the unbalance situation as well as harmonic distortion. These issues can not be reflected into the conventional methodology due to a fixed operating point.

As the increasing number of power electronics system and micro / smart grid condition [1, 11] based on the renewable energy source, it is difficult to assume the constant operation without considering the disturbance from outside and varying operating points. Hence, it is required to have more precise models, which are considering all operating possibilities, instead of using simplified model.

III. HSS MODELING OF COMPONENTS

In order to include the previously introduced time varying point, which is critical to the stability and dynamic performance, the HSS modeling based on the HD method is proposed [20, 24]. In this section, the general modeling procedure is given from the basic modeling to a combined modeling with many components.

A. Basic Modeling Procedure & Principles

To adapt the theoretical proof into the practical power electronics based systems, the overall procedure to derive the HSS modeling is like this.

Step1) It is required to derive a general differential equation of the system into a state space format in order to make a HSS model.

$$\dot{x}(t) = Ax(t) + Bu(t) \qquad (1)$$
$$y(t) = Cx(t) + Du(t)$$

Step2) Equation (1) is still an *LTI* model. Hence, the state variable, state transition matrix (A) and the other related input/output matrixes are also needed to be changed into periodically time varying signals as given in equation (2).

$$\dot{x}(t) = A(t)x(t) + B(t)u(t) \qquad (2)$$
$$y(t) = C(t)x(t) + D(t)u(t)$$

At this point of view, the HD theory [20] and concept should be performed as a first step before the HSS modeling is approached. Even though there are several ways to choose the periodic signals, the well-known Fourier-Series theory is used to improve the mathematical proof of the modeling. The main theorem of the Harmonic domain modeling starts from a periodic signal, which can be represented in the interval $[t_0, t_0 + T]$ by its Fourier series.

$$x(t) = \sum_{k \in \mathbb{Z}} X_k e^{jk\omega_0 t} \qquad (3)$$

when, each Fourier coefficient can be calculated by

$$X_k(t) = \frac{1}{T} \int_{t_0}^{t_0+T} x(t) e^{-jk\omega_0 t} dt \qquad (4)$$

where, $\omega_0 = \frac{2\pi}{T}$ and $t \in [t_0, t_0 + T]$

Then in compact notation form

$$x(t) = \Gamma(t)X \qquad (5)$$

where,

$$\Gamma(t) = [e^{-jh\omega_0 t} \cdots e^{-j2\omega_0 t}, e^{-j\omega_0 t}, 1, e^{j\omega_0 t}, e^{j2\omega_0 t} \cdots e^{jh\omega_0 t}]$$
$$X = [X_{-h}(t) \cdots X_{-1}(t)X_0(t)X_1(t) \cdots X_h(t)]^{\mathrm{T}}$$

In a practical application, the maximum harmonic order to h must be limited.

Step3) According to the Step 2, it is possible to represent the time-domain signals into frequency domain signals using a Fourier series. However, this harmonic domain matrix is not enough to show the dynamic transient performance in the time domain and also in order to derive the frequency impedance response depending on the frequency variation. Hence, it is required to employ the kernel function (e^{-st} *or* $e^{-i\omega t}$) to calculate the transient performance like the Fourier transform or Laplace transform. To show the difference among the principal integral based transformation, it can be compared in (6)-(8). As shown in equation (8), the Fourier series can only give the steady state analysis of the signals. On the contrary, the Laplace and the Fourier transform can derive the transient performance together because these two transformations employ the exponential function as the kernel function (e^{-st} *or* $e^{-i\omega t}$).

Practically, it can bring the summation of the impulse response of the input signal. It can be solved in the various ways like the convolution or the integral based sigma expression. But, the Fourier transform is not enough to represent the real part of the complex signals, because the imaginary part is only considered in the calculation. As a result, the Laplace transform has a better ability to describe the dynamic performance in the

linear time invariant systems. Further, each Fourier series response can be converted into the impulse response by multiplying the Exponentially Modulated Periodic (EMP) signal (e^{st}) as a kernel function. This approach is enough to show the dynamic characteristics of each harmonic component. The summation of these responses can be regarded as the original time domain response of the input signals.

$$F(\omega) = \int_0^\infty f(t) e^{-i\omega t} dt \qquad (6)$$

$$F(s) = \int_0^\infty f(t) e^{-st} dt \qquad (7)$$

$$f(t) = e^{st} \sum_{k \in \mathbb{Z}} Z_k e^{jk\omega_0 t} \qquad (8)$$

Step 4) Based on the basic representation of the EMP signal characteristics, it is also possible to derive the various mathematical expressions like the derivative, integral and the product of two signals in order to make a time varying differential equation of the power converter. The derivative of the time varying signal ($x(t) = \Gamma(t)X$) is like :

$$\dot{x}(t) = \dot{\Gamma}(t)X + \Gamma(t)\dot{X} \qquad (9)$$

Step 5) On the other aspect in the s-domain, it also can be represented as :

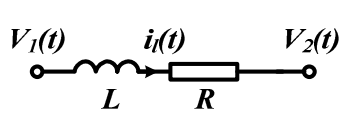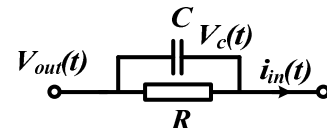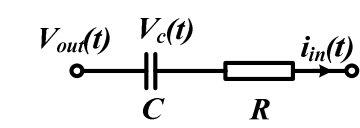$$sX = (A - N)X + BU \qquad (10)$$
$$Y = CX + DU$$

The convolution of the time domain signal is exactly the same with the multiplication of the frequency domain signals and equation (10) can be represented again like the equation (11), where the signals x(t) and u(t) represent the general form of an EMP signal, and the output y(t) also includes the EMP signal terms. It is noticeable that each state variable (x(t)) and state transition matrix (A(t)) are time varying matrix which means that the harmonic frequency component is decomposed by the Fourier series and it can be varied according to the time but periodically. The matrix formation will make it easy to analyze the harmonic coupling and operation point, because each signal is already decomposed into a harmonic component in the time domain. It will also result in the output (Y(ω, t)), which has the decomposed harmonic components.

$$sX(\omega, t) = A(\omega) \otimes X(\omega, t) + B(\omega) \otimes U(\omega, t) \qquad (11)$$
$$Y(\omega, t) = C(\omega) \otimes X(\omega, t) + D(\omega) \otimes U(\omega, t)$$

In terms of the implementation of equation (11), the convolution process can simply be implemented as matrix multiplication. Different with the other modeling methods, the nonlinear components and switching components, which are regarded as time varying systems with periodic excitation, can also be linearized around the nominal frequency like 50 Hz or 60 Hz signals.

Finally, from the principle of these transformation, the state space equation, which has a time varying state transition matrix

Table I. Modeling examples of passive linear components using Harmonic State Space (HSS) modeling

	L-R Series Circuit	R-C Parallel Circuit	R-C Series Circuit
LTI model	$\dot{i}_l(t) = \left[\frac{-R}{L}\right]i_l(t) + \left[\frac{1}{L} \quad -\frac{1}{L}\right]\begin{bmatrix}v_1(t)\\v_2(t)\end{bmatrix}$ $i_l(t) = [1]i_l(t) + [0 \quad 0]\begin{bmatrix}v_1(t)\\v_2(t)\end{bmatrix}$	$\dot{v}_c(t) = \left[\frac{-1}{RC}\right]v_c(t) + \left[\frac{1}{C}\right][i_{in}(t)]$ $v_{out}(t) = [1]v_c(t) + [0][i_{in}(t)]$	$\dot{v}_c(t) = [0]v_c(t) + \left[\frac{1}{C}\right][i_{in}(t)]$ $v_{out}(t) = [1]v_c(t) + [R][i_{in}(t)]$
HSS model	$sX = AX + BU$ $Y = CX + DU$ $A = \begin{pmatrix}-\frac{R}{L} & \cdots & \\ \vdots & \ddots & \vdots \\ & \cdots & -\frac{R}{L}\end{pmatrix} - \begin{pmatrix}-jh\omega0 & \cdots & \\ \vdots & \ddots & \vdots \\ & \cdots & +jh\omega0\end{pmatrix}$ $B = \begin{pmatrix}\frac{1}{L} & \cdots & & \frac{-1}{L} & \cdots & \\ \vdots & \ddots & \vdots & \vdots & \ddots & \vdots \\ & \cdots & \frac{1}{L} & & \cdots & \frac{-1}{L}\end{pmatrix}$ $C = \begin{pmatrix}1 & \cdots & \\ \vdots & \ddots & \vdots \\ & \cdots & 1\end{pmatrix}$ $D = \begin{pmatrix}0 & \cdots & & 0 & \cdots & \\ \vdots & \ddots & \vdots & \vdots & \ddots & \vdots \\ & \cdots & 0 & & \cdots & 0\end{pmatrix}$ $X = [\cdots I_{l-1}, I_{l+0}, I_{l+1} \cdots]^T$ $Y = [\cdots I_{l-1}, I_{l+0}, I_{l+1} \cdots]^T$ $U = [[\cdots V_{1-1}, V_{1+0}, V_{1+1} \cdots][\cdots V_{2-1}, V_{2+0}, V_{2+1} \cdots]]^T$	$A = \begin{pmatrix}-\frac{1}{RC} & \cdots & \\ \vdots & \ddots & \vdots \\ & \cdots & -\frac{1}{RC}\end{pmatrix} - \begin{pmatrix}-jh\omega0 & \cdots & \\ \vdots & \ddots & \vdots \\ & \cdots & +jh\omega0\end{pmatrix}$ $B = \begin{pmatrix}\frac{1}{C} & \cdots & \\ \vdots & \ddots & \vdots \\ & \cdots & \frac{1}{C}\end{pmatrix}$ $C = \begin{pmatrix}1 & \cdots & \\ \vdots & \ddots & \vdots \\ & \cdots & 1\end{pmatrix}$ $D = \begin{pmatrix}0 & \cdots & \\ \vdots & \ddots & \vdots \\ & \cdots & 0\end{pmatrix}$ $X = [\cdots V_{c-1}, V_{c+0}, V_{c+1} \cdots]^T$ $Y = [\cdots V_{out-1}, V_{out+0}, V_{out+1} \cdots]^T$ $U = [\cdots I_{in-1}, I_{in+0}, I_{in+1} \cdots]^T$	$A = \begin{pmatrix}0 & \cdots & \\ \vdots & \ddots & \vdots \\ & \cdots & 0\end{pmatrix} - \begin{pmatrix}-jh\omega0 & \cdots & \\ \vdots & \ddots & \vdots \\ & \cdots & +jh\omega0\end{pmatrix}$ $B = \begin{pmatrix}\frac{1}{C} & \cdots & \\ \vdots & \ddots & \vdots \\ & \cdots & \frac{1}{C}\end{pmatrix}$ $C = \begin{pmatrix}1 & \cdots & \\ \vdots & \ddots & \vdots \\ & \cdots & 1\end{pmatrix}$ $D = \begin{pmatrix}R & \cdots & \\ \vdots & \ddots & \vdots \\ & \cdots & R\end{pmatrix}$ $X = [\cdots V_{c-1}, V_{c+0}, V_{c+1} \cdots]^T$ $Y = [\cdots V_{out-1}, V_{out+0}, V_{out+1} \cdots]^T$ $U = [\cdots I_{in-1}, I_{in+0}, I_{in+1} \cdots]^T$
Block Diagram	$V_1(t)$ — $i_l(t)$ — $V_2(t)$, L R	C $V_c(t)$, $V_{out}(t)$, $i_{in}(t)$, R	$V_{out}(t)$ $V_c(t)$, $i_{in}(t)$, C R

$(A − N)$ and the time varying state variable (X), can be represented as the production of the matrix as like shown in the equation (12).

$$(s + jm\omega_0)X_n = \sum_{-\infty}^{\infty} A_{n-m}X_m + \sum_{-\infty}^{\infty} B_{n-m}U_m \quad (12)$$
$$Y_n = \sum_{-\infty}^{\infty} C_{n-m}X_m + \sum_{-\infty}^{\infty} D_{n-m}U_m$$

B. Passive Components/ Filter connection

To reduce the switching harmonic and in the other distorting harmonic in the *GVSC*, the passive components in a filter connection are also important components. Those components can be represented into the HSS model formation using (9)-(12). The summary of the passive components modeling is shown in Table I. Particularly, in the case of HSS model, it can also include the linearized non-linear inductor or transformer model instead of the linear model through the Newton-Raphson linearization method as shown in (13) [20].

$$[I] = [Y][V] + [I_N] \quad (13)$$
$$[I_N] = [I_b] − [Y][V_b]$$

where, the linearized non-linear admittance matrix (Y), input voltage (V), dependent current (I_N), base voltage (V_b), base current (I_b) and output current (I) derived from the linearized matrix (Y). The derived linearized non-linear inductor information can be replaced with the matrix given in Table I. in order to obtain the non-linear characteristic of output current (I).

$$[Y] = \begin{bmatrix} Y_0 & Y_{-1} & \ddots \\ Y_1 & Y_0 & Y_{-1} \\ \ddots & Y_1 & Y_0 \end{bmatrix} \quad (14)$$

C. Harmonic Transfer of the Switching Elements

In terms of the harmonic transfer procedure between DC and AC, the switching component and modulation technique can be regarded as important components in the *GVSC*. In the conventional modeling and analysis methods [9, 13], the switching term is just modeled as constant gain (V_{dc}/V_{carr}), where the V_{dc} is dc link voltage magnitude and V_{carr} is carrier waveform magnitude. However, the switching components can be decomposed into the Fourier coefficients by means of Fourier series as like equation (3). Practically, the switching component is an important part in terms of the harmonics. As it can transfer harmonics from dc to ac or opposite according to equation (15),

$$V_{out}(t) = s(t)V_{in}(t) \quad (15)$$

where, $V_{out}(t)$ is the output signal, which is derived from the multiplication of the switching term ($s(t)$) and input signal ($V_{in}(t)$). To derive the same result with the time domain multiplication, the convolution in the frequency domain can be considered. The results can easily be obtained through a matrix multiplication. Hence, it is required to change switching instant term ($s(t)$) to the Toeplitz matrix [22], which is composed by the important harmonic terms as given in equation (16).

$$\begin{bmatrix} \vdots \\ V_{out0} \\ \vdots \end{bmatrix} = \begin{bmatrix} S_0 & S_{-1} & \ddots \\ S_1 & S_0 & S_{-1} \\ \ddots & S_1 & \ddots \end{bmatrix} \begin{bmatrix} \vdots \\ V_{in0} \\ \vdots \end{bmatrix} \quad (16)$$

However, the switching harmonic matrix in (16) is also for the fixed reference signal (operating point), the practical reference signal is continuously varying according to the control output. Hence, in order to get a more precise frequency characteristic of the *GVSC*, the critical switching harmonic ($\Gamma[... S_{-1}, S_0, S_1, ...]$) needs to be updated continuously. This can be achieved through the procedure given in Fig. 2.
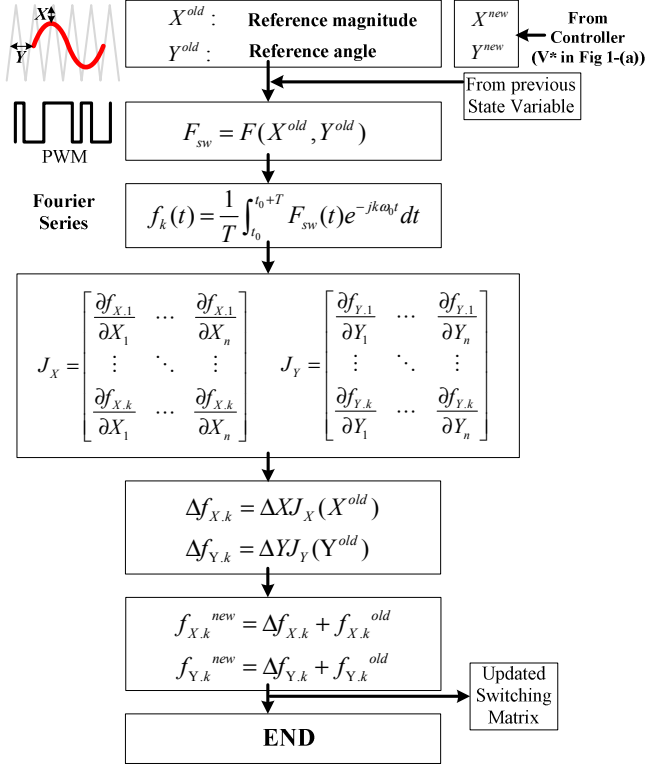

Fig 2. Block diagram for switching harmonic matrix linearization

In Fig. 2, "k" means the harmonic order of the PWM switching signal, which is derived from the Fourier series. The final results from the Fig. 2 block diagram can be updated by means of the Jacobian matrix process, when the reference magnitude and angle are varied by the controller. By adding the derivative terms of the Fourier coefficient components ($\Delta f_{X.k}, \Delta f_{Y.k}$) into the old terms ($f_{X.k}^{old}, f_{Y.k}^{old}$), the updated switching harmonic coefficient terms ($f_{X.k}^{new}, f_{Y.k}^{new}$) can be obtained. The derived switching element from Fig. 2 is linearized switching components, which can be updated in every time when the reference signal is changed. Therefore, it can show time – varying / non-linear switching harmonic component in the linearized model compared to the conventional modeling method [9].

IV. HSS MODELING OF GRID CONNECTED CONVERTER

According to the introduced modeling theory, the HSS modeling for *GVSC* using an *LCL* filter can be derived as shown in Fig. 3.

$$sw(t) = [s_{ab}(t) \quad s_{bc}(t) \quad s_{ca}(t)] \quad (17)$$

$$v_{inv}(t) = sw(t)^T[v_{dc}(t)] \quad (18)$$

$$i_{dc}(t) = sw(t)[i_{ga}(t) \quad i_{gb}(t) \quad i_{gc}(t)]^T \quad (19)$$

$$C_{dc}\frac{dv_{dc}(t)}{dt} = i_{dc}(t) \quad (20)$$

$$v_{g-abc}(t) - v_{cap-abc}(t) = L_g\frac{di_{g-abc}(t)}{dt} + R_g i_{g-abc}(t) \quad (21)$$

$$v_{cap-abc}(t) - v_{inv-abc}(t) = L_f\frac{di_{f-abc}(t)}{dt} + R_f i_{f-abc}(t) \quad (22)$$

$$i_{g-abc}(t) - i_{f-abc}(t) = C_f\frac{dv_{cap-abc}(t)}{dt} \quad (23)$$

where, acronyms can be found in Fig. 1. Based on equation (17) ~ (23), the time-domain state space equation of *GVSC* can be derived as given in (24).

$$\begin{bmatrix} \dot{\iota}_{g-abc}(t) \\ \dot{\iota}_{f-abc}(t) \\ \dot{v}_{cap-abc}(t) \\ \dot{v}_{dc}(t) \end{bmatrix} = \begin{bmatrix} -\frac{R_g}{L_g} & 0 & -\frac{1}{L_g} & 0 \\ 0 & -\frac{R_f}{L_f} & \frac{1}{L_f} & -\frac{sw(t)^T}{L_f} \\ \frac{1}{C_f} & -\frac{1}{C_f} & 0 & 0 \\ 0 & \frac{sw(t)}{C_{dc}} & 0 & 0 \end{bmatrix} \begin{bmatrix} i_{g-abc}(t) \\ i_{f-abc}(t) \\ v_{cap-abc}(t) \\ v_{dc}(t) \end{bmatrix} + $$
$$\begin{bmatrix} \frac{1}{L_g} & 0 & 0 & 0 \end{bmatrix} \begin{bmatrix} v_{g-abc}(t) \\ 0 \\ 0 \\ 0 \end{bmatrix} \quad (24)$$

Through the HSS modeling procedure, which is described in III-A, equation (24) can be transformed to the HSS modeling format as shown (25).

$$\begin{bmatrix} \dot{I}_{g-abc}(t) \\ \dot{I}_{f-abc}(t) \\ \dot{V}_{cap-abc}(t) \\ \dot{V}_{dc}(t) \end{bmatrix} = \begin{bmatrix} \frac{-R_g}{L_g}I - N & 0 & \frac{-1}{L_g}I & 0 \\ 0 & \frac{-R_f}{L_f}I - N & \frac{1}{L_f}I & -\frac{\Gamma[SW^T]}{L_f} \\ \frac{1}{C_f}I & \frac{-1}{C_f}I & -N & 0 \\ 0 & \frac{\Gamma[SW]}{C_{dc}} & 0 & -N \end{bmatrix} \begin{bmatrix} I_{g-abc}(t) \\ I_{f-abc}(t) \\ V_{cap-abc}(t) \\ V_{dc}(t) \end{bmatrix} + $$
$$\begin{bmatrix} \frac{1}{L_g}I & 0 & 0 & 0 \end{bmatrix} \begin{bmatrix} V_{g-abc}(t) \\ 0 \\ 0 \\ 0 \end{bmatrix} \quad (25)$$

where, "*I*" means the identity matrix and "*N*" is the dynamic matrix, which is derived from (9). The time domain switching function is reorganized into a Toeplitz (Γ) [22] matrix in order to perform a convolution by means of the method described in Fig. 2. The small letter in (24) means the time domain signal. On the other hand, the capital letters in (25) stands for the harmonic coefficient component, which is derived from the Fourier series. The results from (25) can be re-transformed into the time
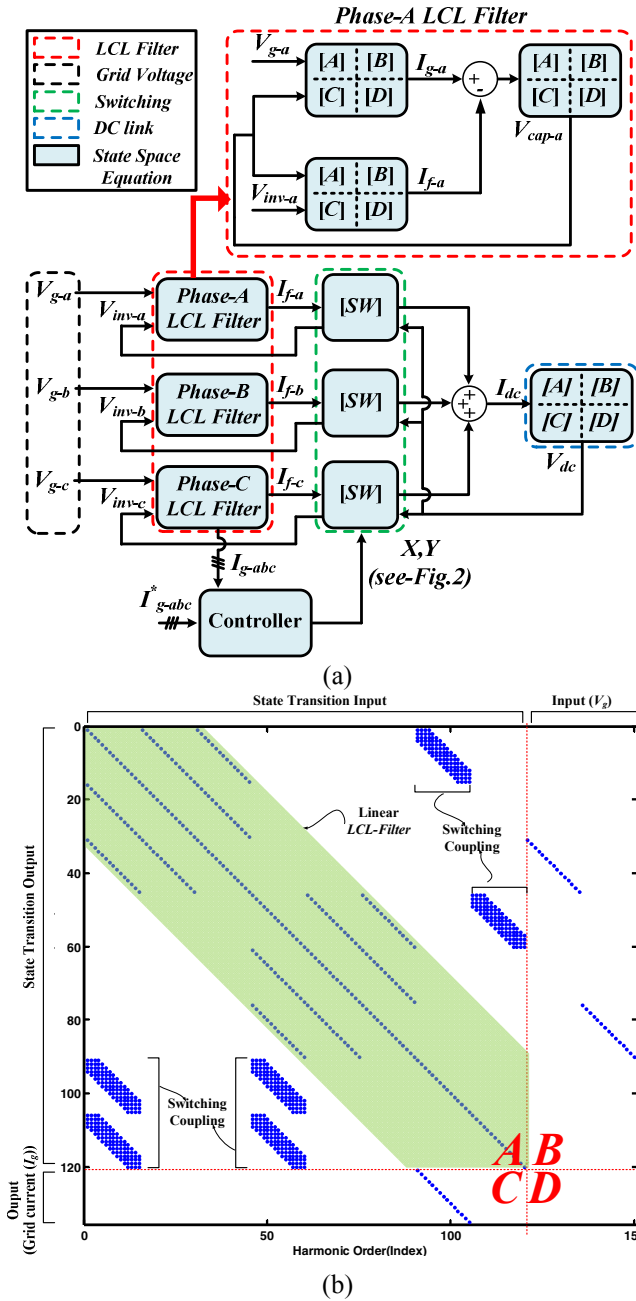
(a)

(b)

Fig 3. HSS modeling of *GVSC* for the k-harmonic order (a) Block diagram of 3-phase grid connected converter with *LCL* filter (b) Full sparse matrix of Phase-A (harmonic = -21th ~21th)

domain signal by means of equation (5) according to the principle of *LTP*.

The number of harmonics is important in terms of accurate time domain simulations, and the procedure is given in Fig. 3-(a). To achieve a more precise model, a full-order harmonic model is unavoidable. However, if only the characteristic harmonics are of interest, then the 3-phase PWM converter switching sequence [27], the positive and negative sequence components can be considered in order to reduce the model order.

The reduced harmonic order HSS model-sparse matrix is shown in Fig. 3-(b), where "Harmonic order (index)" means the harmonic components from negative to positive frequency like [… -h…h…]. The harmonic interaction of all interesting harmonic components can be found in Fig. 3-(b), where the switching component can transfer the harmonic components from ac-side to dc-side or in the opposite way to the time domain.

V. SIMULATION AND EXPERIMENTAL RESULTS

Matlab is used to simulate the analyzed results in time and frequency domain. According to the international standards IEC 61000-2-4, which defines the compatibility levels in industrial plants for low-frequency conducted disturbances and applies for low-voltage and medium voltage at 50 Hz or 60 Hz, distorted grid voltage is simulated with HSS of 3-phase grid connected converter including the *LCL* filter. Laboratory tests are also performed in an experimental set-up, where 3-phase frequency converter is used as the PWM converter. The control algorithms are implemented in a DS1006 dSPACE system. A programmable ac source is also used to make a distorted grid voltage condition.

The verification of the modeling validity is performed under the distorted grid voltage, where the case-A has 3rd (0.5%), 5th (4.5%), 7th (1.5%), the case-B has 2nd (0.2%), 3rd (0.5%), 5th (2.5%), 7th (4.5%) injected into the grid. Besides, in order to compare the HSS modeling simulation results with commercial simulation program, the PLECS is also considered together in order to verify the modeling results. Furthermore, to identify the source of distorted current, the simple PI-controller without harmonic compensator is considered in both simulation and experimental results as shown in Fig 3-(a).

$$\text{HTF}_k(s) = C(sI - A)^{-1}B + D \qquad (26)$$

As shown in Fig. 4, the distorted grid voltage harmonic is transferred through a switching function in Fig. 3-(b). The harmonic impedance elements in the state transition matrix (A), which is including filter and switching, are the most important matrix. Besides, the dynamics of each harmonic can be decided according to the transfer function introduced in (26). If the PWM switching frequency is high, the most critical switching harmonic component is the fundamental terms. However, the switching components harmonics located in the low frequency range can be important in the low switching frequency (< 2 *kHz*). Because, the switching harmonic components in the high switching frequency, are mostly located in the high frequency range but they can be moved to near the low frequency range if
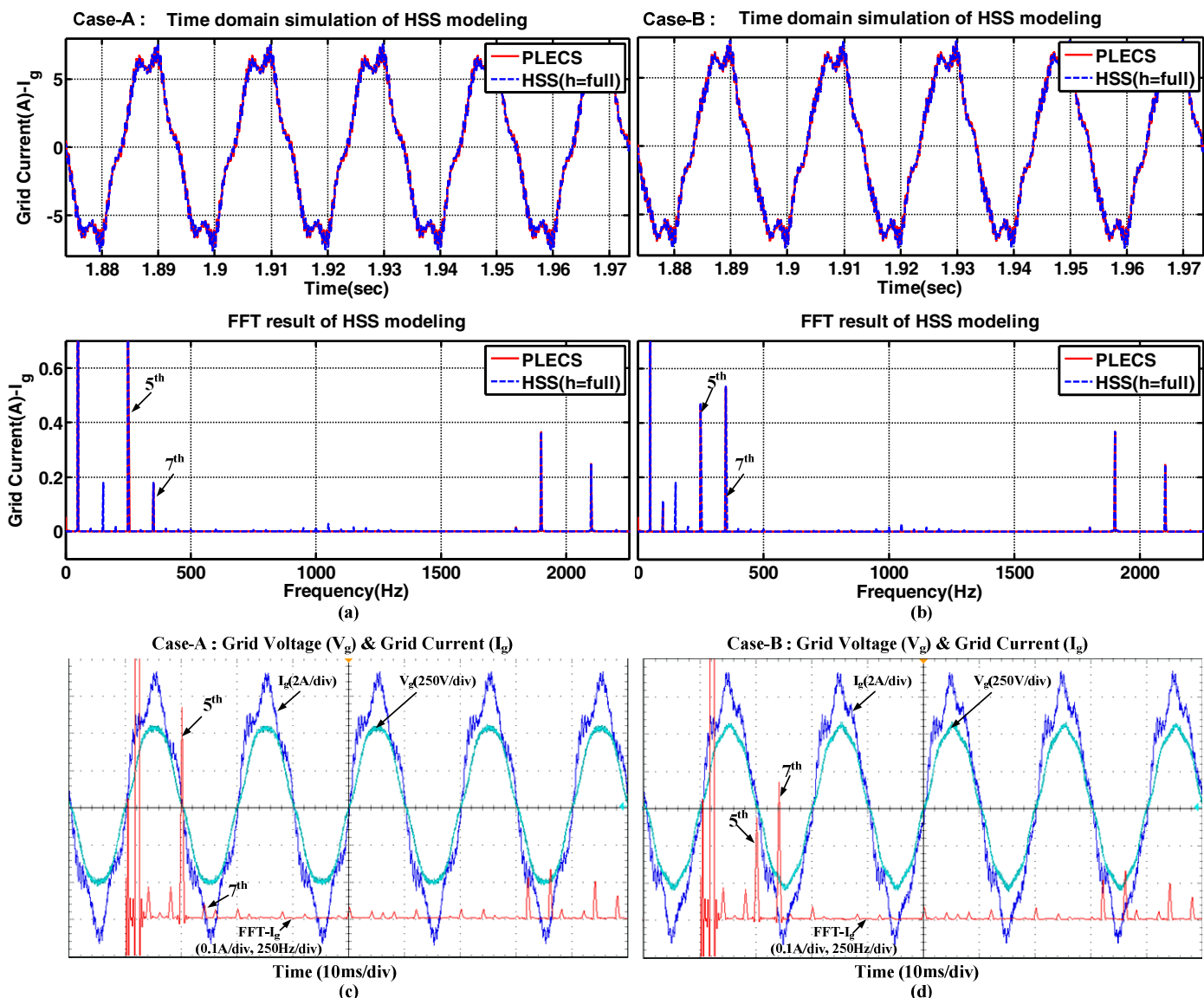
Fig 4. Simulation and experimental results at 3kW Power rating : converter side inductor L_f= 6.25 mH, grid side inductor L_g = 3.3 mH, filter capacitance C_f= 9.4uF, dc link capacitor = 1000 uF, dc link voltage = 750 V, line-line grid voltage = 380 V, switching frequency = 2 kHz)
- Grid side inductor current simulation (harmonic = -40th ~40th) waveform from distorted grid voltage (a) Case-A (b) Case-B- (blue = grid side current, cyan=grid voltage, red = FFT waveform of grid side current)
- Grid side inductor current experiment waveform from distorted grid voltage (c) Case-A, (d) Case-B - (blue = grid side current, cyan=grid voltage, red = FFT waveform of grid side current)

the switching frequency range, which can affect both dc and ac harmonic transfer procedure [27].

In the obtained results, there are differences in both time and frequency domain. The reason is that dead-time, which is generating even-order harmonic, and non-linear characteristic of the inductor are not taken into account in the simulation. If the non-linear passive components are considered, they can be also included in the results. By means of the procedure in Fig 2 and equation (13) with a multi-line diagonal matrix, it can derive the

harmonic, which can not be found in linear passive components. Even though there are differences between simulation and experimental results, the HSS modeling results can show the same capability with non-linear time domain simulation results, where only the linear components are implemented.

VI. CONCLUSION

This paper analyzes the harmonic interaction between grid connected converter and grid network voltage using HSS

modeling. It is verified that the output harmonics, which are derived from input harmonic components and harmonic transfer matrix, is well matched with simulation as well as experimental results. Further, this harmonic impedance matrix can be connected with other harmonic transfer matrix in order to analyze the interaction with other systems because the time and frequency domain results are derived from a coupled matrix.

REFERENCES

[1] J. H. R. Enslin and P. J. M. Heskes, "Harmonic interaction between a large number of distributed power inverters and the distribution network," *IEEE Trans. on Power Electron.,* vol. 19, pp. 1586-1593, 2004.

[2] M. Bollen, J. Meyer, H. Amaris, A. M. Blanco, A. Gil de Castro, J. Desmet*, et al.*, "Future work on harmonics - some expert opinions Part I - wind and solar power," in *Harmonics and Quality of Power (ICHQP), 2014 IEEE 16th International Conference on*, 2014, pp. 904-908.

[3] J. Meyer, M. Bollen, H. Amaris, A. M. Blanco, A. Gil de Castro, J. Desmet*, et al.*, "Future work on harmonics - some expert opinions Part II - supraharmonics, standards and measurements," in *Harmonics and Quality of Power (ICHQP), 2014 IEEE 16th International Conference on*, 2014, pp. 909-913.

[4] X. Wang, F. Blaabjerg, and W. Weimin, "Modeling and Analysis of Harmonic Stability in an AC Power-Electronics-Based Power System," *IEEE Trans. on Power Electron.,* vol. 29, pp. 6421-6432, 2014.

[5] X. Wang, F. Blaabjerg, M. Liserre, C. Zhe, H. Jinwei, and L. Yunwei, "An Active Damper for Stabilizing Power-Electronics-Based AC Systems," *IEEE Trans. on Power Electron.,* vol. 29, pp. 3318-3329, 2014.

[6] S. T. Tentzerakis and S. A. Papathanassiou, "An Investigation of the Harmonic Emissions of Wind Turbines," *IEEE Trans. Energy Conv.,* vol. 22, pp. 150-158, 2007.

[7] A. Petersson, T. Thiringer, L. Harnefors, and T. Petru, "Modeling and experimental verification of grid interaction of a DFIG wind turbine," *IEEE Trans. Energy Conv.,* vol. 20, pp. 878-886, 2005.

[8] L. Shun, H. Qiaohui, and L. Wei-Jen, "A Survey of Harmonic Emissions of a Commercially Operated Wind Farm," *IEEE Trans. Ind. Appl.,* vol. 48, pp. 1115-1123, 2012.

[9] J. Sun, "Small-Signal Methods for AC Distributed Power Systems-A Review," *IEEE Trans. on Power Electron.,* vol. 24, pp. 2545-2554, 2009.

[10] F. Xiaogang, L. Jinjun, and F. C. Lee, "Impedance specifications for stable DC distributed power systems," *IEEE Trans. Power Electron.,* vol. 17, pp. 157-162, 2002.

[11] X. Wang, F. Blaabjerg, and Z. Chen, "Autonomous Control of Inverter-Interfaced Distributed Generation Units for Harmonic Current Filtering and Resonance Damping in an Islanded Microgrid," *IEEE Trans. Ind. Appl.,* vol. 50, pp. 452-461, 2014.

[12] S. Vesti, T. Suntio, J. A. Oliver, R. Prieto, and J. A. Cobos, "Effect of Control Method on Impedance-Based Interactions in a Buck Converter," *IEEE Trans. Power Electron.,* vol. 28, pp. 5311-5322, 2013.

[13] M. Cespedes and S. Jian, "Impedance Modeling and Analysis of Grid-Connected Voltage-Source Converters," *IEEE Trans. on Power Electron.,* vol. 29, pp. 1254-1261, 2014.

[14] S. Jian, "Impedance-Based Stability Criterion for Grid-Connected Inverters," *IEEE Trans. on Power Electron.,* vol. 26, pp. 3075-3078, 2011.

[15] J. Sun, Z. Bing, and K. J. Karimi, "Input Impedance Modeling of Multipulse Rectifiers by Harmonic Linearization," *IEEE Trans. on Power Electron.,* vol. 24, pp. 2812-2820, 2009.

[16] J. Sun and Z. Bing, "Input impedance modeling of single-phase PFC by the method of harmonic linearization," in *Applied Power Electronics Conference and Exposition, 2008. APEC 2008. Twenty-Third Annual IEEE*, 2008, pp. 1188-1194.

[17] K. Ilves, A. Antonopoulos, S. Norrga, and H. P. Nee, "Steady-State Analysis of Interaction Between Harmonic Components of Arm and Line Quantities of Modular Multilevel Converters," *IEEE Trans. Power Electron.,* vol. 27, pp. 57-68, 2012.

[18] Y. Xibo and A. Lovett, "Dc-link capacitance reduction in a high power medium voltage modular wind power converter," in *Proceeding in Power Electronics and Applications (EPE), 2013* 2013, pp. 1-10.

[19] Y. Zhang and Y. Li, "Investigation and Suppression of Harmonics Interaction in High-Power PWM Current-Source Motor Drives," *IEEE Trans. Power Electron.,* vol. PP, pp. 1-1, 2014.

[20] J. Arrillaga and N. R. Watson, "The Harmonic Domain revisited," in *International Conference on Harmonics and Quality of Power, 2008. ICHQP 2008. 13th* 2008, pp. 1-9.

[21] B. Vyakaranam, M. Madrigal, F. E. Villaseca, and R. Rarick, "Dynamic harmonic evolution in FACTS via the extended harmonic domain method," in *Power and Energy Conference at Illinois (PECI), 2010*, 2010, pp. 29-38.

[22] J. R. C. Orillaza and A. R. Wood, "Harmonic State-Space Model of a Controlled TCR," *IEEE Trans. on Power Delivery.,* vol. 28, pp. 197-205, 2013.

[23] J. R. Orillaza, M. S. Hwang, and A. R. Wood, "Switching Instant Variation in Harmonic State-Space modelling of power electronic devices," in *Universities Power Engineering Conference (AUPEC), 2010 20th Australasian*, 2010, pp. 1-5.

[24] G. N. Love, "Small signal modelling of power electronic converters, for the study of time-domain waveforms, harmonic domain spectra, and control interactions," Doctor of Philosophy, Department of Electrical and Computer Engineering, University of Canterbury, 2007.

[25] E. Mollerstedt, "Dynamic Analysis of Harmonics in Electrical Systems," Doctor of Philosophy, Department of Automatic Control, Lund University, 2000.

[26] J. E. Ormrod, "Harmonic State Space Modelling of Voltage Source Converters," Master, Department of Electrical Computer Engineering, University of Canterbury, 2013.

[27] D. G. Holmes and T. A. Lipo, *Pulse Width Modulation For Power Converters-Principle and Practice*: WILEY, 2003.